A Hybrid Fault Diagnosis Method based on SDG and PLS: Tennessee Eastman Challenge Process

Gibaek Lee

Department of Chemical Engineering, Chungju National University, Chungbuk, Korea
(Tel : +82-43-841-5230; E-mail: glee@chungju.ac.kr)

Abstract: The hybrid fault diagnosis method based on a combination of the signed digraph (SDG) and the partial least-squares (PLS) has the advantage of improving the diagnosis resolution, accuracy and reliability, compared to those of previous qualitative methods, and of enhancing the ability to diagnose multiple fault. In this study, the method is applied for the multiple fault diagnosis of the Tennessee Eastman challenge process, which is a realistic industrial process for evaluating process control and monitoring methods. The process is decomposed using the local qualitative relationships of each measured variable. Dynamic PLS (DPLS) model is built to estimate each measured variable, which is then compared with the estimated value in order to diagnose the fault. Through case studies of 15 single faults and 44 double faults, the proposed method demonstrated a good diagnosis capability compared with previous statistical methods.

Keywords: fault diagnosis, signed digraph, partial least-squares, Tennessee Eastman challenge process

1. INTRODUCTION

Because of the many serious accidents which have been occurred in the history of the chemical process industry, safety has become a top priority for those companies concerned. Such accidents result in an economic loss of over $16 billion/year for the petrochemical industry in the U.S. [6]. The impact of such accidents on the economy includes costs of several billion dollars due to personal injuries, loss of production, and reduction in market share for the companies involved. Therefore, the safe and reliable operation of their chemical processes has become one of the primary concerns of chemical companies attempting to survive in the highly competitive international market.

For the above reasons, automatic fault diagnosis systems are very much in demand, to help operators with decision-making and to keep these operations running continuously, whilst being both efficient and safe. Such systems are used to analyze process data on-line, monitor process trends, and diagnose faults when an abnormal situation arises. Among a variety of fault diagnosis approaches for chemical processes, rule-based expert system, state estimation such as observer and Kalman filter, SDG, qualitative simulation, statistical method, and neural network have been developed [1]. These methods are broadly classified as those that use a process model, and those that rely on process history data. They can be further subclassified as qualitative or quantitative. Our previous study suggested the hybrid method combining SDG and the partial least squares (or projection to latent structures, PLS) [5]. The target system is decomposed based on the local causal relationships of each measured variable in the SDG classified as the qualitative model-based methods. For each decomposed subprocess, local fault diagnosis is performed using the PLS classified as a quantitative history data-based method. The method has the advantages of improving the diagnosis resolution and accuracy compared to previous qualitative methods. Moreover, it enhances the reliability of the diagnosis for all predictable faults, including multiple fault. Although it is based on statistical process data, it allows the diagnosis model to be built based on easily obtainable data sets, and does not require faulty case data sets.

The Tennessee Eastman (TE) process created by the Eastman Chemical Company has been widely used as a benchmark process for evaluating process diagnosis methods (Fig. 1) [3]. Chiang et al. reviewed the fault detection and diagnosis method of the multivariate statistics such as PCA, FDA, PLS, and CVA (canonical variate analysis), and compared them using the case studies of the TE processes [2]. This study considers the multiple fault diagnosis of the TE process using the hybrid fault diagnosis method of system decomposition and DPLS proposed in our previous study. Through the diagnosis result of 15 single faults defined in the TE process, the diagnostic performance is compared with the results of Chiang et al.

2. TENNESSEE EASTMAN PROCESS

2.1 Process Description

Downs and Vogel proposed the TE process and described it in detail [3]. It provides a realistic industrial process for evaluating process control and monitoring methods (Fig. 1). The process is based on a simulation of an actual industrial process where the components, kinetics, and operating conditions have been modified for proprietary reasons. The process has five major units, a reactor, condenser, recycle compressor, vapor/liquid separator, and product stripper, and eight components, A, B, C, D, E, F, G, and H. The gaseous reactants A, C, D, and E, and the inert B, are fed to the reactor where the liquid products G and H are formed. The reactions in the reactor are:

$A(g) + C(g) + D(g) \rightarrow G(liq)$, product 1,
$A(g)+C(g)+E(g)\rightarrow H(liq)$, product 2,
$A(g)+E(g)\rightarrow F(liq)$, byproduct,
$3D(g)\rightarrow 2F(liq)$, byproduct.

The reactions are irreversible, exothermic, and approximately first-order with respect to the reactant concentrations. The reaction rates are Arrhenius functions of temperature where the reaction for G has a higher activation energy than the reaction for H, resulting in a higher sensitivity to temperature. The reactor product stream is cooled through a partial condenser and then fed to a vapor-liquid separator. The vapor exiting the separator is recycled to the reactor feed through a compressor. A portion of the recycle stream is purged to keep the inert and byproduct from accumulating in the process. The condensed components from the separator (stream 10) are pumped to a stripper. Stream 4 is used to strip the remaining reactants from stream 10, which are combined with the recycle stream via Stream 5. The products G and H exiting the base of the stripper are sent to a downstream process.

The process contains 41 measured and 12 manipulated

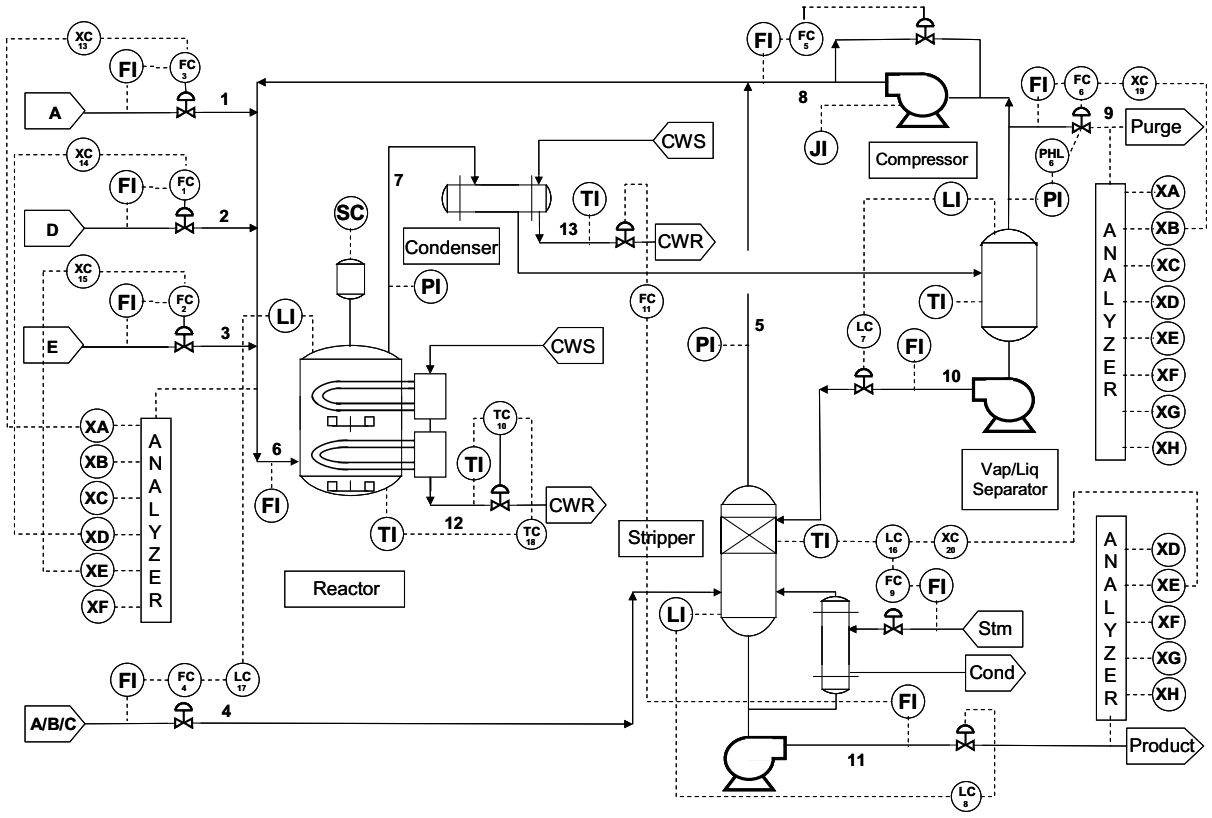

Fig. 1. Process flow diagram of the TE process.

variables. Twenty-two measured variables, F1 through T22, are sampled every minute. Nineteen composition measurements of XA through ZH are taken from streams 6, 9, and 11. The sampling interval and time delay for streams 6 and 9 are both 6 minutes, and for stream 11 are 15 minutes. All the process measurements include Gaussian noise. The TE process simulation contains 21 preprogrammed faults, 16 of which are known, and 5 are unknown. IDV1 through IDV7 are associated with a step change in a process variable. IDV8 through IDV12 are associated with an increase in the variability of some process variables. IDV13 is a slow drift in the reaction kinetics, and IDV14, IDV15, and IDV21 are associated with sticking valves.

The TE simulation Fortran code used in this study can be downloaded from http://brahms.scs.uiuc.edu. A 1-second integration interval is used here. Chiang et al. use a sampling interval of 3 minutes, but this study uses a sampling interval of 1 minute to obtain faster diagnosis results.

Table 1 Faults defined in the TE process.

fault ID	description	type
IDV1	A/C Feed Ratio	Step
IDV2	B Composition	Step
IDV3	D Feed Temp.	Step
IDV4	Reactor CW Inlet Temp.	Step
IDV5	Condenser CW Inlet Temp.	Step
IDV6	A Feed Loss	Step
IDV7	C Header Pressure Loss	Step
IDV8	A, B, C Feed Composition	Random Variation
IDV9	D Feed Temperature	Random Variation
IDV10	C Feed Temperature	Random Variation
IDV11	Reactor CW Inlet Tem.	Random Variation
IDV12	Condenser CW Inlet Temp.	Random Variation
IDV13	Reaction Kinetics	Slow Drift
IDV14	Reactor CW Valve	Sticking
IDV15	Condenser CW Valve	Sticking

2.2 Diagnosis model description

The system is decomposed from the SDG of the TE process. However, it is a very difficult task to build an accurate SDG, because the process contains 4 reactions and 8 components. Especially, the vapor/liquid equilibrium in the reactor, vapor/liquid separator, and stripper becomes a great obstacle in determining the signs of the causal relationships between process variables. However, our method does not need the SDG of the whole process, and uses only the locally reduced SDG of the measured variables, which are directly affected by the faults defined in the process. For these reasons, the efforts to build SDG are greatly reduced. The proposed method can diagnose only the pre-defined faults. Fifteen faults of IDV1 through IDV15 among the 20 faults defined in the simulation program are known. Our study aimed to diagnose these 15 faults (Table 1), and found 26 measured variables directly affected by them. ZD through ZH among the 26 variables are removed, because their sample intervals of 15 minutes are too wide to be helpful in diagnosis speed. This study found that P16 in the simulation program does not mean the stripper pressure, but the pressure of the feed mixing zone. As P16 does not have an accurate value, it is eliminated from the diagnosis. As a result, the process is decomposed centering on 20 measured variables and the reduced digraph for the decomposed subprocess is obtained. The measured variables connected to each measured variable are shown in Table 2, and the faults added to each measured node are shown in Table 3.

In Table 2, the measured variables affecting P7 are

Table 2 Input variables, number of PCs, and time delays.

	input variables for the estimation model	PC	*l*
F1	MV3	1	1
F4	MV4	1	1
P7	F1, F2, F3, F4, F5, L8, T9, P13, F17, YA, YB, YC, YD, YE, YF, YG, YH	10	2
L8	F1, F2, F3, F4, F5, P7, T9, P13, F14, F17, YA, YC, YD, YE, YF, YG, YH	6	1
T9	F1, F2, F3, F4, F5, P7, L8, T11, P13, F17, T18, YA, YB, YC, YD, YE, YF, YG, YH, MV10	6	2
T11	F1, F2, F3, F5, P7, L8, T9, F10, L12, P13, F14, F17, YA, YB, YC, YD, YE, YF, YG, YH, MV11	11	2
P13	F1, F2, F3, F4, F5, P7, L8, T9, F10, T11, L12, F14, F17, YA, YB, YC, YD, YE, YF, YG, YH	9	2
T18	F4, T11, F14, L15, F17, F19, ZD, ZE, ZF, ZG, ZH	8	2
T21	L8, T9, MV10	4	2
T22	T9, MV11, P713	1	1
XA	F1, F2, F3, F4, F5, F17, YA	7	2
XB	F1, F2, F3, F4, F5, F17, YB	7	2
XC	F1, F2, F3, F4, F5, F17, YC	5	1
YA	F5, F6, P7, L8, T9, F10, T11, L12, XA, XC, XD, XE	6	1
YC	F5, F6, P7, L8, T9, F10, T11, L12, XA, XC, XD, XE	7	2
YD	F5, F6, P7, L8, T9, F10, T11, L12, F14, XA, XC, XD	6	1
YE	F5, F6, P7, L8, T9, F10, T11, L12, F14, XA, XC, XE	6	1
YF	F5, F6, P7, L8, T9, F10, T11, L12, F14, XA, XC, XE, XF	7	1
YG	F5, F6, P7, L8, T9, F10, T11, L12, F14, XA, XC, XD	7	1
YH	F5, F6, P7, L8, T9, F10, T11, L12, F14, XA, XC, XD	9	1

originally 13: F5, F6, L8, T9, P13, XA, XB, XC, XD, XE, XF, YG, and YH. However, because the sample interval of XA through XF is as wide as 6 minutes, it is doubtful whether they can represent timely the effect from F1, F2, F3, and F4. Therefore, the reduced digraphs of XA through XF are built, and XA through XF are replaced with F1, F2, F3, F4, F5, F14, F17, and YA through YF. Due to this replacement, IDV1, IDV2, and IDV3 become the faults added to P7. F6 is removed from the estimation model because it can be represented by F1, F2, F3, F4, F14, and F17. For the same reasons, the reduced digraphs of L8, T9, T11, and P13 are changed as shown in Table 2.

The learning data to build the DPLS model for the decomposed subprocess can be obtained in the presence of set-point change or external disturbances. However, the data set in the presence of external disturbance cannot be used because the changes of the operation conditions such as the feed composition and cooling water temperature are not available in the simulation program. In order to get the learning data, the set-point is changed. The set-points of 11 control loops in the TE process can are changed, and the changes are set on the basis of $\pm 10\%$. The set-points of 5 loops are changed to the values lower than $\pm 10\%$ due to the controller outputs saturations when the change is $\pm 10\%$.

The simulation time for the training data set was 10 hours,

Table 3 Fault added to the measured node.

measured variable	sign of arc	
	negative (-)	positive(+) or negative(-)
F1	IDV6	
F4	IDV7	
P7		IDV13
L8		IDV13
T9		IDV3, IDV4, IDV9, IDV11, IDV13, IDV14
T11		IDV5, IDV12, IDV13, IDV15
P13		IDV13
T18		IDV1, IDV2, IDV8, IDV10, IDV13
T21		IDV4, IDV11, IDV14
T22		IDV5, IDV12, IDV15
XA		IDV1, IDV2, IDV8
XB		IDV2, IDV8
XC		IDV1, IDV2, IDV8
YA-YH		IDV13

and the set point was changed after 1 simulation hour from the run. The total number of samples generated for each run was 11×10×60=6600. In considering the time delays, the composition measurement variables having the known time delays of 6 (or 15) minutes show the previous value of 6 (or 15) minutes ago. Therefore, the DPLS models should be modified to deal with this dead time. For instance, XA and YA have the known time delay of 6 minutes. If the current and one previous values are used as input data of the DPLS model, the input X for the estimation of XA(t) is F1(t-6), F2(t-6), F3(t-6), F4(t-6), F17(t-6), YA(t), XA(t-6), F1(t-6), F2(t-6), F3(t-6), F4(t-6), F17(t-6), and YA(t-6). Also, the input X for the estimation of T18(t-15) is F4(t-15), T11(t-15), F14(t-15), L15(t-15), F17(t-15), F19(t-15), ZD(t), ZE(t), ZF(t), ZG(t), ZH(t), T18(t-16), F4(t-16), T11(t-16), F14(t-16), L15(t-16), F17(t-16), F19(t-16), ZD(t-1), ZE(t-1), ZF(t-1), ZG(t-1), and ZH(t-1).

The number of past values l and PCs are determined from the learning data. As in our previous model, this study uses the cross-corelation plots of the scores to determine the number of time lags and PCs, as suggested by Ku et al. [4]. The number of time lags and PCs for the TE process are shown in Table 3. The same data are used to determine the CUSUM parameters of minimal jump size and threshold size.

Using Table 3, the fault sets for the TE process are obtained as shown in Table 4. If a fault occurs, the qualitative state for the residual may be (+) or (-). However, the sign of the arc from the faults to the measured variables are unknown except IDV6 and IDV7 among 15 faults defined in the TE process (Table 3). As the type of IDV8 through IDV12 are random variation, the signs of the symptoms can fluctuate between (+) and (-), which greatly decreases the diagnosis accuracy. In order to consider the characteristics of the faults defind in the TE process and make a stable diagnosis, the diagnosis strategy is modified for CUSUM to monitor the squared residuals as well as the residuals of each variable, according to the following equation:

$$r_i^2 = (y_i - \hat{y}_i)^2 \quad (1)$$

When the symptoms of squared residuals are used, a particular strategy is used to increase the diagnosis speed. In considering the variable of which the squared residual is monitored, if the residual (either + or -) or the squared residual for the variable is detected by CUSUM, it is concluded that

Table 4 Fault sets of the TE process.

symptom	fault set
F1(-)	IDV6
F4(-)	IDV7
P72	IDV1, IDV2, IDV8, IDV13
L82	IDV1, IDV2, IDV8, IDV13
T92	IDV1, IDV2, IDV3, IDV4, IDV8, IDV9, IDV11, IDV13, IDV14
T112	IDV1, IDV2, IDV5, IDV8, IDV12, IDV13, IDV15
P132	IDV1, IDV2, IDV8, IDV13
T182	IDV1, IDV2, IDV8, IDV10, IDV13
T212	IDV4, IDV11, IDV14
T222	IDV5, IDV12, IDV15
XA2	IDV1, IDV2, IDV8
XB2	IDV2, IDV8
XC2	IDV1, IDV2, IDV8
SUMY2	IDV13

the symptom of the squared residual is detected.

The 8 composition measurement variables of YA through YH are affected only by IDV13, and are independent of other faults. It cannot be said that the possibility of false detection of one variable among the 8 variables is low. When each composition variable is monitored separately, false detection of one variable may make the diagnosis unstable. In order to resolve the difficulty, YA through YH are grouped into one variable as follows:

$$SUMY2 = \sum_{i=A}^{H} (Y_i - \hat{Y}_i)^2 \qquad (2)$$

3. EXAMPLE

3.1 IDV1 (A/C Feed Ratio, B Composition Constant)

When the fault occurs, a step change is induced in the A/C feed ratio in stream 4, which decreases the A feed in stream 6 and a control loop reacts to increase the A feed in stream 1. The variations in the flowrate and compositions of stream 6 to the reactor causes variations in the reactor level, which affects the flow rate in stream 4 through a cascade control loop. Since the ratio of the reactants A and C changes, the variables associated with the reaction (level, pressure, and composition) changes correspondingly.

The simulation time for the faulty data set was 48 hours to compare the diagnosis result with that of Chiang et al.'s study. The simulations started with no faults, and the faults were introduced to the run from 8 simulation hours. To measure the diagnostic performance, four parameters were used: accuracy, resolution, wrong detection, and detection delay [3]. The accuracy is 1 if the diagnosis is accurate; that is, the true fault is included in the final fault candidates set. Otherwise, the accuracy is 0. The resolution denotes the number of final fault candidates. Wrong detection refers to the number of falsely detected symptoms independent of the true solution. The detection delay refers to the time from fault occurrence to fault diagnosis, and a short detection delay indicates quick detection and diagnosis.

Fig. 2 shows the residuals of the detected. The bounds of Fig. 2 are the minimal jump size of CUSUM (6σ of the residual distribution). The detection sequence of symptoms are as follows: XA^2 at 522 minutes, $T9^2$ and T9(-) at 532 minutes, XA(-) at 540 minutes, XC(+) from 576 to 2562 minutes (fluctuation), XC^2 at 600 minutes, P7(+) from 616 to 940

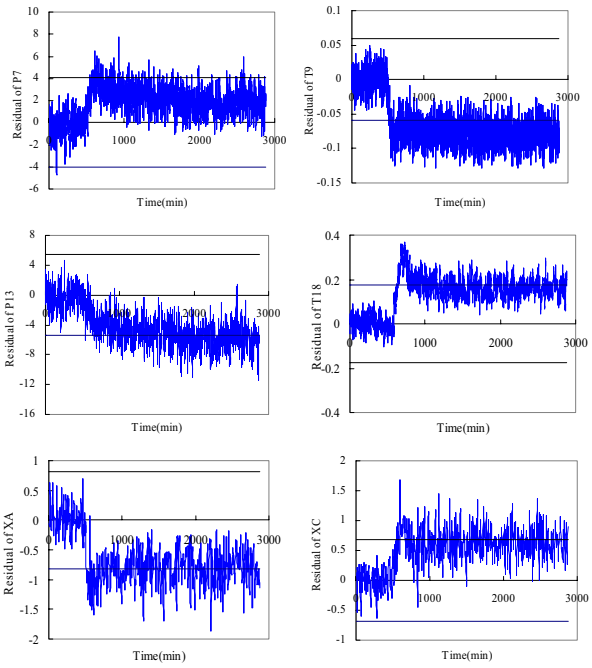

Fig. 2. Residuals of the detected variables for IDV1.

minutes (fluctuation), $P7^2$ from 618 to 1093 minutes, $T18^2$ at 694 minutes, T18(+) from 699 to 1204 minutes, P13(-) at 1036 minutes (fluctuation), and $P13^2$ at 1037 minutes.

The symptoms having sign are XA(-), XC(+), T18(+), T9(-), P7(+), and P13(-). The fault candidates are IDV1, IDV2, and IDV8 from 522 minutes to the last diagnosis time. The symptom of $F1^2$ is falsely detected at 571, 572, and 1676 minutes, and $F4^2$ at 1905 and 1906 minutes. Although the final fault candidates obtained for these 5 minutes of false detection are 6 double faults including IDV6 or IDV7, the final solution does include the true solution and the accuracy is 1 from the detection to the last diagnosis time. The fluctuation of XC(+), P7(+) and P13(-) between detection and missed detection does not have any effect on the accuracy. The accurate symptom of XA^2 is detected at 42 minutes from the fault occurrence and the detection delay is 42 minutes. As the final fault candidates are IDV1, IDV2, and IDV8, the resolution is 3.

The definition of IDV1 does not include the sign of the fault. However, we can see that the symptoms of XA(-) and XC(+) indicate the decrease of the A/C feed ratio in stream 4. Therefore, IDV1 plus A/C feed ratio(-) can be a more accurate solution. When IDV2 occurs, B composition change and A/C feed ratio is constant, indicating that the sign of the symptoms of XA and XC should be the same regardless of B composition. This is a potential diagnosis strategy to increase the diagnosis resolution.

3.2 IDV11 (Reactor Cooling Water Inlet Temperature)

IDV11 induces a fault in the reactor cooling water inlet temperature. The fault in this case is a random variation. The fault induces large oscillations in the reactor cooling water flow rate, which results in a fluctuation of reactor temperature.

Fig. 3 shows the residuals and squared residuals of the detected variables. The bounds of Fig. 6 are the minimal jump size of CUSUM (6σ of the residual distribution). The detection sequence of symptoms is T21(+) at 498 minutes (fluctuation), $T21^2$ at 502 minutes, T21(-) at 533 minutes (fluctuation), and T9(+), T9(-), and $T9^2$ during 228 minutes

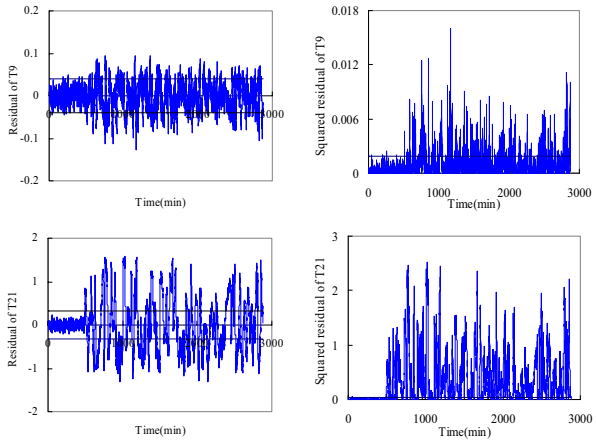

Fig. 3. Residuals and squared residuals of T9 and T21 for IDV11.

from 660 to 2874 minutes. The detection of T9(+), T9(-), T21(+) and T21(-) are fluctuating between detection and missed detection. If the diagnosis uses only residuals, the stable solution cannot be obtained. However, as the squared residuals are used, a stable solution is obtained from the detection to the last diagnosis time. There is no false detection in this case. IDV4, IDV11, and IDV14 are obtained as the solution, and the resolution is 3. Also, the detection delay of 18 minutes is better than the best result (21 minutes) of Chiang et al.

4. RESULT

4.1 Result of single fault cases

Table 5 shows the obtained diagnosis result, and compares the result with that of Chiang et al. The wrong detection and resolution shown in this table is the average of the one measured every 1 minute from the initial detection time to the last diagnosis time. The value in brackets refers to the worst result obtained during all diagnostic periods. Chiang et al. compared various statistical methods such as PCA, DPCA, CVA, PLS, FDA, and DFDA. In Table 5, the left and right values of the slash in the result of Chiang et al. refer to the best and worst results of these methods, respectively.

Table 5 Diagnosis results for single faults.

	detection delays (min)		accuracy		
	linear PLS	Ching et al	linear PLS	Chiang et al. (best/worst)	
				missed detection	misclassi-fication
IDV1	42	6/21	1	0/0.01	0.01/0.88
IDV2	115	36/75	1	0.01/0.03	0.01/0.44
IDV3	-	-	0	0.98/0.99	0.73/1
IDV4	2	3/-	1	0/0.98	0.12/1
IDV5	13	0/48	1	0/0.78	0.006/1
IDV6	1	0/33	1	0/0.01	0/0.83
IDV7	1	0/3	1	0/0.49	0/0.98
IDV8	90	60/69	0.61	0.02/0.49	0.00/1
IDV9	-	-	0	0.981/0.994	0.77/1
IDV10	189	69/303	1	0.1/0.67	0.1/1
IDV11	18	21/912	1	0.19/0.80	0.12/0.99
IDV12	68	0/66	0.99	0/0.029	0.01/0.99
IDV13	142	111/147	1	0.04/0.06	0.21/1
IDV14	11	3/18	1	0/0.16	0.00/0.99
IDV15	-	2031/-	0	0.9/0.99	0.73/1

When Chiang et al. considered detection delays, a fault was indicated only when six consecutive measure values have exceeded the threshold, and the detection delay was recorded as the first time instant in which the threshold was exceeded. Therefore, it is expected that the actual detection delay of their method will be more than the detection delay shown in Table 5. The detections of five cases (IDV4, IDV6, IDV7, IDV11, and IDV14) are faster than those of Chiang et al. Also, the other cases show similar or only slightly worse detection delays than their methods.

The diagnosis for three cases (IDV3, IDV9, and IDV15) failed because the fault sizes of these cases were so small and therefore the variations of process variables were as weak as the steady state. Therefore, other methods used by Chiang et al. also encounter difficulty in making accurate diagnosis (Table 5).

In the other 12 cases, except IDV8, the diagnostic accuracies are almost 1 during all diagnosis periods. In the diagnosis of IDV8, our method failed during 39.1% of the diagnosis periods, and the accuracy is 0.609. The symptoms of P7, T9, P13, and XA are detected, but are frequently missed due to the small fault size, indicating that the diagnostic performance of the suggested method depends on the fault size. However, the key symptom of IDV8, XA^2, is detected during 31 minutes from 570 minutes, and this time of 31 minutes should be sufficient to decide the fault occurrence. The parameters of the missed detection and misclassification rates used by Chiang et al. mean the diagnosis failure rate. Although the meaning is not the same, the difference in value of one and two parameters can be a comparable value with the accuracy used in this study. In most cases, the accuracy obtained by our study was one, which was better than the result obtained by Chiang et al.

In the diagnosis of IDV6, the average wrong detection was over 7. This is due to the controller output saturations, such as MV3 (547 minutes, 100%), MV9 (764 minutes, 100%), MV10 (1037 minutes, 100%), MV5 (1152 minutes, 100%), MV6 (1225 minutes, 0%), and MV4 (1303 minutes, 100%), and the fact that the operation range guided by the fault is very different from that of the training data.

4.2 Result of double fault cases

Double faults are generated from the combinations of single faults. As IDV3, IDV9, and IDV15, among 15 single faults, have a detection problem, they are omitted in the combinations for double faults. IDV6 is also omitted because it makes a number of false detections. Fifty-five double faults from 11 single faults ($_{11}C_2$) can be made. However, the proposed method cannot diagnose double faults which affect the same measured variables. For instance, the symptoms set which can be generated from IDV2 or IDV8 includes all possible symptoms from IDV1. With the double faults of IDV1 and IDV2, the possible solutions are IDV1, IDV2, and IDV8. Therefore, 11 double faults are removed and 44 double faults are tested. Table 6 shows the diagnosis for double fault cases.

In Table 6, the resolutions of two cases are low. The accuracy of the double fault of IDV2 and IDV12 is very low with the average value of 0.106. In this case, SUMY2 was wrongly detected during 2112 minutes, and XA and XB were detected in short periods. As IDV13 can explain one more symptom than IDV2, the diagnosis failed. In the case of IDV5 and IDV10, the average accuracy is 0.073. As the symptoms

Table 6 Diagnosis results for double faults.

first fault	second fault	detection delay	accuracy	wrong detection	resolution	first fault	second fault	detection delay	accuracy	wrong detection	resolution
IDV1	IDV4	42/2	1	0.005(1)	8.918(9)	IDV5	IDV10	13/187	0.073	0(0)	7(7)
	IDV5	12/12	0.998	0(0)	10.88(11)		IDV11	13/17	1	0.005(2)	20.98(21)
	IDV7	30/1	0.9996	0.006(1)	2.967(3)		IDV13	13/13	0.980	0.033(2)	7.705(12)
	IDV11	42/18	1	0.005(1)	8.954(9)		IDV14	12/9	1	0.005(1)	20.98(21)
	IDV12	42/118	0.999	0.025(2)	8.99(11)	IDV7	IDV8	1/90	0.999	0.052(1)	3.350(9)
	IDV13	42/846	0.999	0.006(1)	3.162(8)		IDV10	1/184	0.9996	0(0)	4.696(5)
	IDV14	42/12	1	0.005(1)	8.924(9)		IDV11	1/18	1	0.003(1)	2.986(3)
IDV2	IDV4	115/2	1	0(0)	11.54(12)		IDV12	1/31	0.985	0.128(1)	3.271(7)
	IDV5	12/12	1	0.0006(1)	10.23(12)		IDV13	1/147	0.9996	0.155(1)	1.965(4)
	IDV7	116/1	0.807	0.007(1)	3.807(4)		IDV14	1/16	1	0.0004(1)	2.988(3)
	IDV11	112/18	1	0.001(0)	11.61(12)	IDV8	IDV11	90/18	1	0.005(1)	8.787(12)
	IDV12	77/77	0.106	0.183(1)	7.184(12)		IDV12	68/68	0.925	0.018(2)	11.59(27)
	IDV13	183/183	0.944	0.003(1)	3.089(8)		IDV13	90/145	0.784	0.303(2)	3.848(5)
	IDV14	113/16	1	0(0)	11.58(12)		IDV14	90/11	1	0.003(1)	9.365(12)
IDV4	IDV5	2/13	1	0.004(0)	20.92(21)	IDV10	IDV11	188/18	1	0.0004(1)	14.14(15)
	IDV7	2/1	1	0.002(1)	2.999(3)		IDV12	184/68	0.855	0.005(1)	13.56(15)
	IDV8	2/90	1	0.005(1)	7.824(12)		IDV14	189/11	1	0.0004(1)	14.11(15)
	IDV10	2/189	1	0(0)	14.06(15)	IDV11	IDV12	18/68	0.954	0.015(1)	9.876(21)
	IDV12	2/68	0.972	0.033(1)	10.13(21)		IDV13	18/141	1	0.008(1)	5.591(12)
	IDV13	2/142	1	0.007(1)	5.581(12)	IDV12	IDV13	68/68	0.997	0.028(1)	4.154(12)
IDV5	IDV7	12/1	1	0.01(1)	6.706(7)		IDV14	68/11	0.946	0.012(1)	10.16(21)
	IDV8	13/13	0.999	0.009(1)	9.861(27)	IDV13	IDV14	141/11	1	0.007(1)	5.455(12)

of T11 and T18 were detected to the last and T22 was not detected, single faults of IDV1, IDV2, IDV8, and IDV13 can explain two symptoms of T11 and T18 during long diagnosis periods.

Wrong detections are less than 1 on average. In Table 6, resolution is not low because a number of single faults that affect the same measured variables can be distinguished only by the fault type of step and random variation.

5. CONCLUSION

This study investigated the multiple fault diagnosis of the TE process, which is a benchmark process for evaluating process diagnosis methods. The hybrid diagnosis method combining SDG and DPLS, proposed in our previous study, was used. The process was decomposed centering on 20 measured variables which are directly affected by the 15 faults defined in the TE process, and the reduced digraph for the decomposed subprocess was made. Dynamic linear PLS model was constructed for each decomposed subprocess, and fault diagnosis was performed by using the residual between the estimated value determined by the DPLS model and the measured one.

Through the case studies of 15 single faults, the diagnosis performance was compared with the statistical methods reviewed by Chiang et al., which need faulty case data sets. The result confirmed that the satisfactory accuracy of the proposed method. Especially, the diagnosis of five cases by the proposed method was faster than that by other methods. The average wrong detection of one single fault case was over 7, because the operation range guided by the fault was very different from that of the training data. For further study, the diagnosis strategy will have to be able to change the DPLS models according to the significant changes of the operation ranges. If sufficient data for various operation ranges are provided, multivariate statistics such as PCA can be helpful to judge the change of the operating conditions. After the estimation models are switched, the CUSUM parameters of minimal jump size and threshold size may be changed. Also, the change needs a strategy to smoothly alter the variables of the detection program. Double fault diagnosis of the TE process was performed. The diagnosis results were acceptably accurate.

ACKNOWLEDGMENTS

This work was supported by grant No. (R05-2002-000-00057-0) from the Basic Research Program of the Korea Science & Engineering Foundation

REFERENCES

[1] W.R. Becraft, D.Z. Guo, P.L. Lee, R.B. Newel, "Fault Diagnosis Strategies for Chemical Plants: A Review of Competing Technologies," *Proceedings of PSE '91*, pp 12.1-12.15, **1991**.

[2] L.H. Chiang, E.L. Russell, and R.D. Braatz, *Fault Detection and Diagnosis in Industrial Systems*, Springer, London, 2001.

[3] J.J. Downs and E.F. Vogel, "A Plant-wide Industrial Process Control Problem," *Comput. Chem. Eng.*, Vol. 17, pp. 245-255, **1993**.

[4] W. Ku, R.H. Storer, and C. Georgakis, "Disturbance Detection and Isolation by Dynamic Principal Component Analysis," *Chemometrics Intell. Lab. Syst*., Vol. 30, pp. 179-196, **1995**.

[5] G. Lee, S-O., Song, and E.S. Yoon, "Multiple-Fault Diagnosis Based on System Decomposition and Dynamic PLS," *Ind. Eng. Chem. Res.,* Vol. 42, pp. 6145-6154, **2003**.

[6] I., Nimmo, "Adequately Address Abnormal Operations," *Chem. Eng. Progress*, Sep, pp. 36-45, **1995**.